IEEE Access
Multidisciplinary | Rapid Review | Open Access Journal

Received 23 May 2024, accepted 28 June 2024, date of publication 2 July 2024, date of current version 16 July 2024.

Digital Object Identifier 10.1109/ACCESS.2024.3422313

RESEARCH ARTICLE

A Novel Deep Learning Approach for Accurate Cancer Type and Subtype Identification

JABED OMAR BAPPI[1], MOHAMMAD ABU TAREQ RONY[2], MOHAMMAD SHARIFUL ISLAM[3], SAMAH ALSHATHRI[4], AND WALID EL-SHAFAI[5,6], (Senior Member, IEEE)

[1]Department of Electrical and Electronics Engineering, Port City International University, Chittagong, 4225 Bangladesh
[2]Department of Statistics, Noakhali Science and Technology University, Noakhali 3814, Bangladesh
[3]Department of Computer Science and Telecommunication Engineering, Noakhali Science and Technology University, Noakhali 3814, Bangladesh
[4]Department of Information Technology, College of Computer and Information Sciences, Princess Nourah Bint Abdulrahman University, P.O. Box 84428, Riyadh 11671, Saudi Arabia
[5]Security Engineering Laboratory, Computer Science Department, Prince Sultan University, Riyadh 11586, Saudi Arabia
[6]Department of Electronics and Electrical Communication Engineering, Faculty of Electronic Engineering, Menoufia University, Menouf 32952, Egypt

Corresponding authors: Mohammad Abu Tareq Rony (rony1513@student.nstu.edu.bd), Samah Alshathri (sealshathry@pnu.edu.sa), and Walid El-Shafai (eng.waled.elshafai@gmail.com)

This work was supported by Princess Nourah Bint Abdulrahman University, Riyadh, Saudi Arabia, through the Researchers Supporting Project under Grant PNURSP2024R197.

ABSTRACT Cancer is a disease where abnormal cells grow uncontrollably and spread to other body parts. It can originate anywhere in the human body, which consists of trillions of cells. These cells continually divide, replenishing the body's needs. As cells age or sustain damage, they naturally undergo apoptosis, allowing new cells to take their place. Our research uses a secondary dataset from Kaggle, comprising over 130,000 images representing various cancer types. We have developed a novel Deep-learning model capable of detecting and classifying cancer at early stages with remarkable accuracy. The model classifies eight primary cancer types and 26 subtypes, each represented by 5,000 images. Our approach combines various computational tools, including pre-trained Convolutional Neural Networks, Machine learning, and Deep learning classifiers such as KNN and SVM, and innovative multimodal architectures of merged CNN-LSTM hybrids. We applied two distinct classification strategies. In our first approach, the main class and subclass are classified together. In the second approach, the model first predicts the main eight classes and then 26 subclasses concerning the main class classification, where the KNN model achieved higher accuracy for the Lymphoma class than CNNs. Finally, the X-OR gate-based fusion technique applied after prediction significantly reduces misclassifications and enhances the certainty of cancer types. Our findings reveal great accuracy levels of 99.25% for primary cancer classifications and 97.80% for subclass classifications. The introduction of novel models, Vception (VGG + Inception) and Vmobilnet (VGG + MobileNet), integrated with LSTM, further advances diagnostic capabilities. Again, By utilizing an X-OR gate post-prediction from Vmobilenet and Vception models, we achieved a main class accuracy of 99.95% and a subclass accuracy of 99.13%, significantly boosting model confidence. Moreover, individually, KNN achieved 97.14% accuracy for the Lymphoma class using PCA. This study not only sets a new benchmark in cancer detection but also promises to improve patient care and treatment outcomes significantly.

INDEX TERMS Cancer detection, deep learning, cancer imaging, CNNs, misclassifications, PCA.

I. INTRODUCTION

Cancer stands as a significant challenge in the domain of global health, responsible for almost 10 million deaths each year. This severe and intricate illness arises when regular cells mutate into malignant forms. Such mutations are the consequence of complex interactions between genetic factors inherent to the individual and external environmental influences. The progression of cancer involves multiple phases, starting with the emergence of pre-cancerous conditions and eventually leading to the growth of invasive tumors [1].

The associate editor coordinating the review of this manuscript and approving it for publication was Carmelo Militello.

In developing countries, cancer mortality remains a significant challenge for humanity [2]. Despite the availability of numerous preventive measures, some types of cancer still lack effective treatments. Cancer mortality represents a critical concern within the healthcare sector, notably as a leading cause of death among women. Early detection of brain cancer is essential for effective treatment. Brain tumors are diagnosed through biopsies, a process requiring invasive brain surgery. However, computational intelligence techniques offer a non-invasive alternative, assisting physicians in identifying and classifying brain tumors [3].

Automatic detection of leukemia is a vital process in early medical diagnosis and treatment planning and presents a formidable challenge in healthcare. Leukemia, a blood cancer originating in the bone marrow, primarily affects white blood cells (WBCs), disrupting normal blood function [4]. A cost-effective and minimally invasive method, microscopic analysis of WBCs is widely recognized for the early identification of this hematological disorder. Despite its importance, there has been a scarcity of extensive literature reviews on the application of deep and Machine Learning(ML) techniques specifically for Acute Lymphoblastic Leukemia (ALL) detection, a gap that underscores the need for more thorough research in this critical area of medical technology [5].

Breast cancer is the most prevalent form among women and particularly affects those with denser breast tissue due to physiological characteristics [6]. Early detection of this disease is crucial in reducing the mortality rate. According to Globocan 2018 data, breast cancer accounts for one in every four cancer diagnoses in women globally and is the fifth leading cause of death worldwide [7].

Cervical cancer, predominantly affecting women, is a globally recognized health concern. It arises from the abnormal proliferation of cells in the cervix and can gradually extend to other body organs [8]. If identified early, cervical cancer is entirely treatable. There are several screening techniques for this disease, yet early detection through cost-effective Pap smear tests is crucial for a successful cure [9].

The kidneys function as the body's filtration system, eliminating unwanted or harmful substances while recirculating essential nutrients such as vitamins, amino acids, glucose, and hormones into the bloodstream. Research indicates that kidney cancer ranks as the 13th most prevalent cancer worldwide, and among men, it is the 9th most common. In 2012, there were 214,000 new cases in men and 124,000 in women. In the United States, kidney tumors represent approximately 3.7% of all cancer diagnoses. Annually, over 62,000 Americans are diagnosed with one of the 4,444 types of kidney cancer [10].

Colon and lung cancer have emerged as significant contributors to disability and mortality worldwide. The histopathological examination of these cancers plays a crucial role in identifying the best treatment approach. Early and prompt diagnosis significantly reduces the risk of death from these diseases. Advanced technologies, such as Deep Learning(DL) and ML, are being employed to accelerate the detection of these cancers. These methods enable the medical research community to evaluate a larger number of patients more quickly and cost-effectively [11].

Cervical lymphadenopathy frequently occurs in children. Currently, there is no established decision model for identifying high-grade Lymphoma in pediatric patients with this condition. While previous research has pinpointed specific predictive factors for Lymphoma, and a small number have developed multivariate models, none have achieved the discriminative power necessary for practical clinical use [12].

Oral cancer stands as one of the leading cancer types worldwide, with late detection significantly contributing to increased morbidity and higher mortality rates. Roughly 50% of all oral cancer cases are identified in South Asia, and about two-thirds of cases arise in low- and middle-income nations. The predominant causes of oral cancer are extensive alcohol use and tobacco smoking. The survival rates for oral cancer are notably low in these regions, primarily because approximately two-thirds of affected individuals in low- and middle-income countries present with oral lesions at advanced stages, hindering effective treatment outcomes [13].

Molecular imaging allows for the observation and quantitative evaluation of changes in biological processes at the molecular and/or cellular scale, offering crucial insights into early cancer detection [14]. In contemporary medical imaging analysis, DL has emerged as a prevalent method, surpassing conventional ML and visual assessment constraints by extracting intricate hierarchical features with robust representational capacity. There's a dynamic surge in cancer molecular image research employing DL methodologies [15]. The following are the main contributions of this research work:

- As all of the previous research focuses on single cancer classes, we proposed a novel method to tackle eight main cancer classes and 26 sub-classes concurrently, offering a comprehensive understanding of cancer types.
- We introduce two novel innovative convolutional neural network architectures, VCEPTION (combining VGG and Inception) with LSTM and VMOBILENET (combining VGG and MobileNet) with LSTM, to elevate model performance in multicancer image classification.
- Finally, a novel fusion approach is applied where we introduce X-OR gate integration in two independently trained models post-prediction, we ensure precise disease classification, advancing diagnostic accuracy and clinical decision-making in cancer imaging.

The organization of this paper is as follows: Section II reviews the relevant literature. Section III introduces our novel method for cancer detection. Section IV evaluates the results of different deep learning techniques. Finally, Section V summarizes our research findings.

II. LITERATURE REVIEW

The ongoing research focuses on using DL techniques to diagnose various cancers from image datasets. Recent studies have aimed to develop ML models for accurate and early cancer detection. The use of DL techniques to analyze radiographic images for cancer detection and classification has become increasingly popular. This section provides a detailed review of DL methods used for diagnosing cancers, along with a comparative analysis summarized in Table 1.

This study [16] tackles early detection by proposing a sophisticated deep-learning algorithm that scrutinizes white blood cells using microscopic blood smear images. ALL is a critical cancer predominantly found in children, characterized by the overproduction of lymphocytes. The novel algorithm is based on a Convolutional Neural Networks(CNNs), aptly named ALLNET, which distinguishes leukemic cells from non-cancerous ones. The research utilized a publicly accessible dataset of microscopic images for training and validating the ALLNET model. The training was executed on Google Collaboratory, harnessing the computational power of Nvidia Tesla P-100 GPUs. The model excelled, attaining an accuracy of 95.54%, specificity of 95.81%, sensitivity of 95.91%, F1-score of 95.43%, and precision of 96%. These results underscore the model's potential as a pre-screening tool for leukemia in blood tests, significantly aiding in the early and accurate detection of ALL.

The study [17] focuses on classifying brain tumor types from MRI images using an enhanced DL approach, specifically employing Residual Networks. The objective is to develop a Computer Assisted Diagnosis (CAD) system to aid doctors and radiologists in accurate tumor diagnosis and classification. The benchmark dataset consists of 3064 MRI images encompassing three brain tumor types: Meningiomas, Gliomas, and Pituitary tumors. Through rigorous evaluation, the proposed model achieves a remarkable 99% accuracy, surpassing previous methodologies. In addition to accuracy, the study employs other metrics such as precision, recall, f1-score, and balanced accuracy to address imbalanced dataset challenges, ensuring robust performance in tumor classification.

The research [18] addresses the challenging task of breast cancer detection, considering its significant impact as a leading cause of female cancer mortality. Introducing the DL-assisted Efficient Adaboost Algorithm (DLA-EABA), the research employs advanced computational techniques to enhance breast cancer classification. It explores the utilization of deep CNNs for tumor classification across various imaging modalities like MRI, ultrasound, digital breast tomosynthesis, and mammography. The DL framework integrates convolutional layers, Long Short-Term Memory(LSTM), and max-pooling layers, culminating in a fully connected layer and softmax layer for classification and error estimation. By combining ML approaches with feature selection and extraction methods, the study achieves impressive accuracy levels of 97.2%, sensitivity of 98.3%, and specificity of 96.5%, outperforming existing systems.

The article in [19] aims to improve cervical cancer screening through computer-assisted diagnosis. By developing a method that combines low- and high-resolution whole slide images (WSIs) for lesion cell recognition and a neural network-based model for WSI classification, the research achieves high specificity (93.5%) and sensitivity (95.1%) in slide classification. Tested on 1,170 patient-wise WSIs, the system outperforms three cytopathologists on average. It also highlights the top 10 lesion cells with an 88.5% true positive rate on 447 positive slides. Post-deployment, the system can recognize one giga-pixel WSI in about 1.5 minutes, promising efficient and accurate cervical cancer screening.

The research [20] introduces computational techniques for kidney segmentation in CT images, crucial for disease diagnosis and treatment planning. Manual segmentation is time-consuming and subject to variability, prompting the adoption of deep CNNs. The proposed method combines image processing and CNNs to minimize false positives. Using the KiTS19 dataset, our approach achieved outstanding results: Dice coefficient of 96.33%, Jaccard index of 93.02%, sensitivity of 97.42%, specificity of 99.94%, and accuracy of 99.92%. In the KiTS19 challenge, it attained a Dice coefficient of 93.03%. These findings underscore the efficacy of our method, showcasing its potential for precise kidney segmentation in CT imaging, aiding in early tumor detection and clinical decision-making.

This paper [21] introduces a novel training strategy for accurate segmentation of sparsely annotated histopathological data and proposes a transfer learning scenario for precise classification of colorectal images. Leveraging pre-trained DL models from computer vision datasets addresses the challenge of limited annotations in whole-slide images (WSIs). Various state-of-the-art CNNs are reviewed and compared, including AlexNet, VGG, ResNet, DenseNet, and Inception models. Transfer learning utilizes features learned from ImageNet to enhance classification accuracy. Testing on the AiCOLO colon cancer dataset yields impressive results, with ResNet achieving up to 96.98% accuracy. Additionally, pixel-wise segmentation strategies employing UNet and SegNet models showcase significant improvements, with SegNet achieving up to 81.22% accuracy. Evaluation of CRC-5000, nct-crc-he-100k, and Warwick datasets demonstrates the robustness of the proposed methods. This study provides valuable insights into effective network selection and training strategies for colon tumor segmentation in histopathological images.

This study [22] addresses the challenge of diagnosing hematopoietic malignancies through diagnostic histopathology, requiring labor-intensive slide reading with near-perfect accuracy. Despite AI's assistance, achieving clinically usable diagnostic accuracy remains elusive due to dataset size and variation handling requirements. The research establishes a highly accurate DL platform using smaller datasets, focusing

on human diffuse large B-cell Lymphoma (DLBCL) and non-DLBCL images from three hospitals. Multiple classify pathologic images with near-perfect accuracy (100% for hospital A, 99.71% for hospital B, and 100% for hospital C). While technical variability initially affects cross-hospital performance, eliminating it maintains 100% diagnostic accuracy. This work demonstrates the clinical practicality of utilizing DL models for DLBCL diagnosis and potentially other hematopoietic malignancies.

The objective of this study [23] is to develop a lightweight deep CNN tailored for binary classification of oral lesions as either benign or malignant/potentially malignant using real-time clinical images. A small CNN leveraging a pre-trained EfficientNet-B0 model is proposed. Training and testing are conducted using a dataset of 716 clinical images. Performance evaluation metrics include accuracy, specificity, sensitivity, receiver operating characteristics (ROC), and area under curve (AUC). The proposed CNN model achieves promising results, with an accuracy of 85.0%, specificity of 84.5%, sensitivity of 86.7%, and AUC of 0.928. These findings suggest that deep CNNs can effectively support the development of low-cost embedded vision devices for oral cancer diagnosis, thereby enhancing the quality and accessibility of oral cancer screening and early detection.

A. RESEARCH GAP AND QUESTIONS

In the field of early detection of cancer, the literature review identifies a significant research gap in the domain of multi-cancer detection, particularly in multiple classes and subclasses at the same time, classification accuracy, adaptability, and efficiency. Our research addresses two primary research questions we have identified from literature analysis:

- Our proposed novel model can simultaneously detect multiple types of cancer, enhancing the scope of diagnosis of multi-cancer and potentially improving the efficiency of cancer screening processes.
- Our study investigates the most fruitful ML and DL approaches for the efficient detection of multiple cancers.

To bridge this gap, our paper introduces an advanced technique. Our novel method aims to enhance accuracy and efficiency, catering to the detection of Cancer. By integrating diverse CNNs and DL techniques, the proposed novel method offers an efficient and robust solution in the evolving landscape of Cancer detection.

III. PROPOSED METHODOLOGY

In this section, we first explain the dataset used in this study and the image preprocessing methods we applied to the dataset. We then propose our novel approach by integrating CNN models and LSTM to enhance multicancer detection and classification, specifically VCEPTION (VGG + Inception) and VMOBILENET (VGG + MobileNet) for our merged CNN with LSTM framework. We also introduce the Exclusively-OR(X-OR) gate as post-processing step to leverage the combined strengths of individual models. Finally, we propose a fusion of CNN, LSTM, and K-Nearest Neighbors(KNN) models including the integration of Principal Component Analysis(PCA) to improve lymphoma cancer subclass classification.

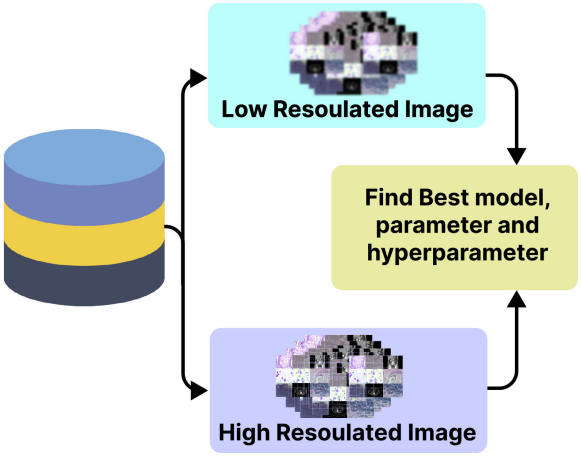

FIGURE 1. Dataset selection.

A. MULTICANCER IMAGE DATASET

In this research, we conducted a comprehensive analysis of two distinct Multicancer image datasets sourced from Kaggle [24]. The first dataset consists of seven main classes and 23 subclasses, while the second dataset comprises eight main classes and 26 subclasses shown in Table 2. The list of the main classes and their subclasses is given in Table 3. A notable disparity between these datasets lies in the resolution of the images, with the first dataset containing lower-resolution images compared to the higher-resolution images present in the second dataset.

Our approach involved initially focusing on fine-tuning our models and optimizing hyperparameters using the lower-resolution dataset, as depicted in Figure 1. This decision was primarily driven by computational constraints. Processing over 100,000 images from the higher-resolution dataset would have imposed substantial demands on GPU resources and time. By starting with the lower-resolution dataset, we aimed to streamline our experimentation process, iteratively refining our models and methodologies before scaling up to the higher-resolution dataset.

To facilitate our analysis, we strategically selected representative samples from each dataset to ensure adequate coverage of the main classes and subclasses. This sampling strategy allowed us to maintain a balanced distribution of classes and subclasses while mitigating the computational burden associated with processing large datasets.

Moving forward, we plan to utilize the insights gained from our experimentation with the lower-resolution dataset to inform our approach to the higher-resolution dataset. By establishing a robust foundation with the lower-resolution data, we aim to optimize our models' performance and

TABLE 1. Summary of recent studies on cancer research.

Ref	Year	Cancer Types	Objectives	Dataset	Methods	Results
[16]	2022	ALL	Detection of ALL	Microscopic Blood smear images	ALLNET model integrated with CNN	95.54% accuracy
[17]	2020	Brain Tumors	CAD system development	3064 MRI images	Enhanced DL with Residual Networks	99% accuracy
[18]	2020	Breast Cancer	Enhance breast cancer classification	Various modalities	DLA-EABA with CNNs	97.2% accuracy, 98.3% sensitivity, 96.5% specificity
[19]	2021	Cervical Cancer	Improve cervical cancer screening	1,170 WSIs	Low- and high-resolution WSIs combination	93.5% specificity, 95.1% sensitivity
[20]	2020	Kidney Segmentation	Disease diagnosis and planning	KiTS19 dataset	Image processing and CNNs	Dice coefficient of 96.33%
[21]	2021	Colorectal Cancer	Accurate segmentation of WSIs	AiCOLO, CRC-5000, others	Transfer learning with CNNs	Up to 96.98% accuracy with ResNet
[22]	2020	Lymphoma	Diagnose DLBCL and non-DLBCL	Images from three hospitals	Multiple CNNs	Near-perfect accuracy (100%)
[23]	2022	Oral Lesions	Classify lesions using clinical images	716 clinical images	Pretrained EfficientNet-B0	85.0% accuracy, 86.7% sensitivity, AUC of 0.928

TABLE 2. Dataset information.

Dataset Name	Main Class	Sub Class	Total Images
Lower Res. Image	7	23	110,000
Higher Res. Image	8	26	130,002

generalizability before transitioning to the more complex and computationally intensive task of working with higher-resolution images.

B. IMAGE PROCESSING TECHNIQUES

To enhance the quality and features of the multicancer images, a series of image processing techniques were applied. Morphological operations were applied to refine the representation of cancerous regions. Erosion reduced noise and fine-tuned object boundaries, while dilation enlarged boundaries and connected broken structures, enhancing the overall image quality. Subsequently, image enhancement techniques, including histogram equalization and contrast stretching, were employed to improve visibility and aid feature extraction. Gaussian blur is a low-pass filtering technique, that was then applied to reduce noise and emphasize important features [25]. The blurring operation contributed to the overall smoothing of the images, preserving essential structures. Finally, Fourier transforms analysis [26] was applied to gain insights into the frequency domain, providing a representation of image features. The segmentation process, utilizing contour detection, highlighted relevant regions of interest, contributing to the overall understanding of the multicancer dataset. Figure 2 shows different types of image processing that are applied in multicancer image datasets.

C. ENHANCING CANCER DETECTION THROUGH CNN-LSTM INTEGRATION

CNNs, drawing inspiration from the hierarchical structure of the human brain, have revolutionized the way we process complex image data [27]. The architecture of CNNs shown in Figure 3, characterized by its convolutional layers, pooling operations, and fully connected layers, forms the bedrock of our methodological approach [28]. By meticulously analyzing medical images through multiple filters, CNNs can detect subtle cues indicative of cancerous changes, thus providing a robust framework for early detection [29]. Beyond spatial analysis, understanding temporal and sequential data is paramount in the medical field. LSTM networks shown in Figure 4, a sophisticated variant of recurrent neural networks (RNNs), offer a window into the temporal dynamics of cancer progression. LSTMs are adept at handling sequences of data, making them ideal for analyzing series of medical images or patient histories to detect patterns or changes over time that may indicate the onset of cancer.

In our study, we innovatively combine CNNs with LSTM networks. The fusion of these technologies creates a robust framework for evaluating medical images, significantly enhancing the precision of cancer detection by leveraging the distinct advantages of each approach for a holistic analysis. This hybrid approach ensures a thorough examination of cancer-related imagery by evaluating both the spatial details and the temporal progression of potential cancerous formations. The integration strategy involves placing the LSTM units after the convolutional layers, as depicted in Figure 5, thereby facilitating a deeper and more understanding of the data. This figure illustrates the seamless integration of a CNN with an LSTM unit, showcasing how this combination can significantly enhance the model's ability to identify and classify cancerous lesions by effectively leveraging spatial and temporal data dimensions.

1) EXPLORING THE MERGE CNNS

Our novel approach involves merging CNNs, where multiple CNNs are combined, and their outputs are merged after

TABLE 3. Main cancer classes and subclasses.

Main Cancer Class	Subclass Name
Acute Lymphoblastic Leukemia (ALL)	ALL Benign ALL Pre ALL Pro ALL Early
Brain Cancer	Brain Glioma Brain Meningioma Brain Tumor
Breast Cancer	Breast Benign Breast Malignant
Cervical Cancer	Cervical Dysplasia (DYK) Cervical Kocytosis (KOC) Cervical Metaplasia (MEP) Cervical Papilloma (Pab) Cervical Squamous Intraepithelial Lesion (SFI)
Kidney Cancer	Kidney Normal Kidney Tumor
Colon Cancer	Colon Adenocarcinoma (ACA) Colon Benign Tumor (BNT)
Lymphoma	Chronic Lymphocytic Leukemia (CLL) Follicular Lymphoma (FL) Mantle Cell Lymphoma (MCL)
Oral Cancer	Oral Normal Oral Squamous Cell Carcinoma (SCC)

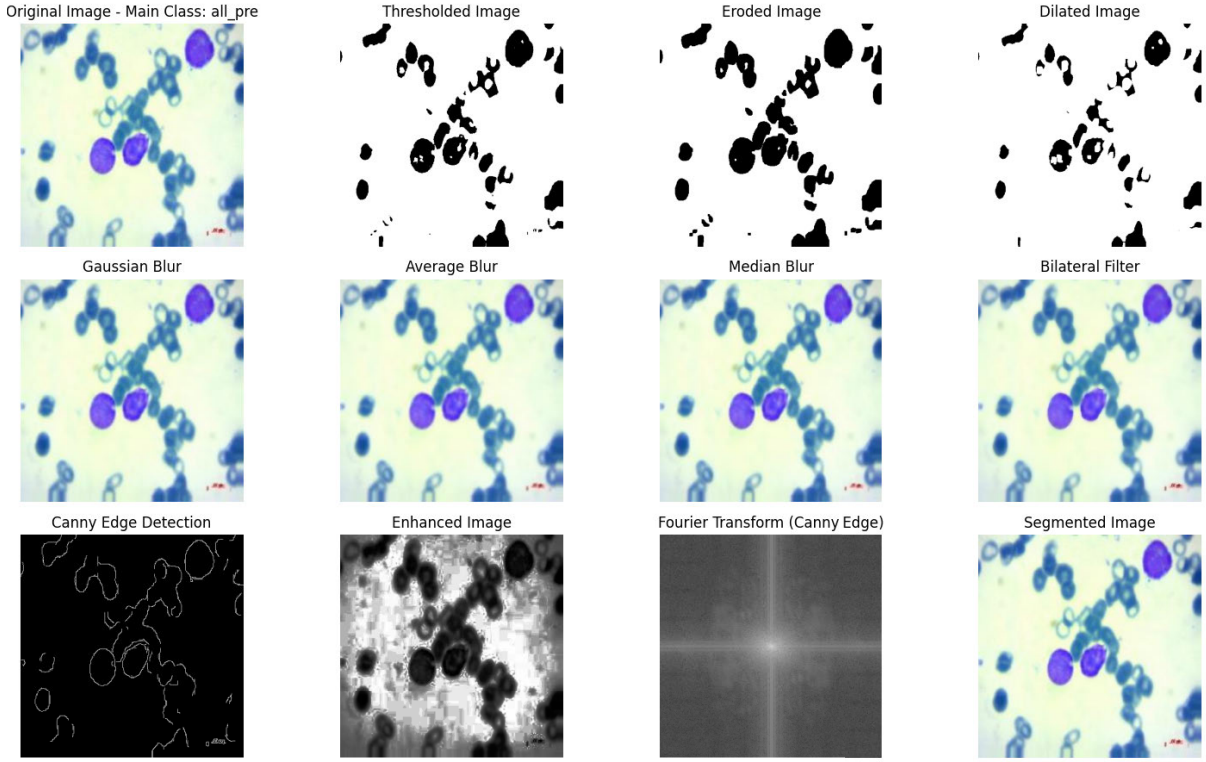

FIGURE 2. Combined image processing steps for cancer detection.

convolution and flattening. This strategy enriches the model's understanding by providing a holistic view of the patient's condition, thereby enhancing the accuracy of cancer detection. In the merge CNN framework, as illustrated in Figure 6, each input image passes through multiple CNNs separately, and their outputs are merged, typically through concatenation or addition, before proceeding with further convolutional layers. By integrating multiple CNNs within the merge framework, our model can effectively capture complementary features from various modalities or perspectives, leading to more robust and accurate predictions in multiple cancer detection tasks.

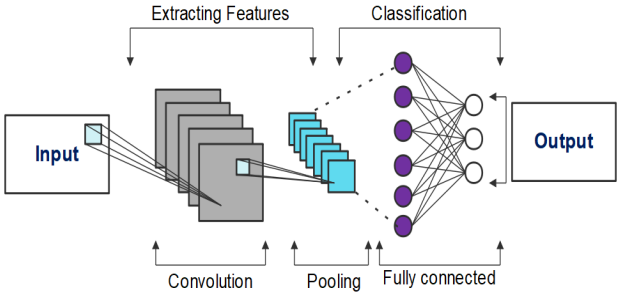

FIGURE 3. Fundamentals of CNN architecture.

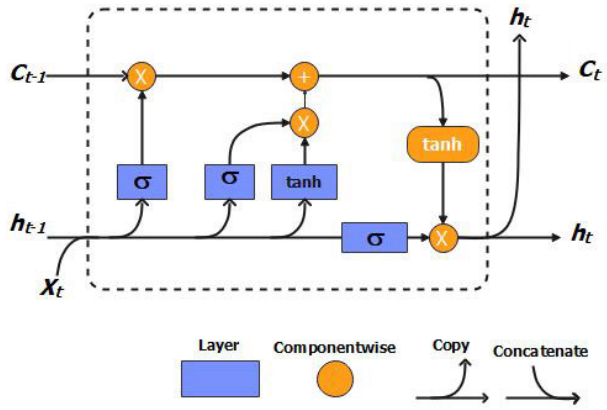

FIGURE 4. Intricacies of LSTM architecture.

2) MULTIMODAL FUSION WITH LSTM

In this variant, our exploration extends to a multimodal CNN architecture, integrating different pre-trained CNNs where the input data consists of images. The incorporation of LSTM units further augments the model's ability to grasp the temporal dynamics inherent in multimodal information. This enhancement results in improved performance, particularly for tasks demanding a comprehensive understanding of diverse data sources. Following the LSTM layer, a dense layer and dropout are applied to mitigate overfitting.

D. PROPOSED NOVEL MODEL

Our proposed methodology for multicancer image classification, illustrated in Figures 7 and 8, involves a comprehensive approach aimed at detecting both main classes and subclasses.

Figure 7 represents our first strategy, where we initially conduct model training on the lower-resolution dataset to identify the most effective model. Subsequently, we apply this optimized model to the higher-resolution dataset for improved accuracy and performance. In strategy one, the focus is primarily on classifying the main classes. Once a main class is identified, we further classify the subclass with respect to the main class. For instance, if the main class is classified as LYMPHOMA, we apply PCA and KNN techniques. On the other hand, if the main class is different, we use a different CNN-LSTM model and classify the subclass accordingly.

Figure 8 represents the second strategy, where the model classifies the main and subclass together. After this classification, we select the two best models. Then, we apply the XOR gate operation to these two models. If both models predict the same output, we consider this classification. However, if the two models predict different outputs, we skip the image. This approach ensures a more precise classification by considering the agreement between the two models.

For tighter classification, we partition the dataset into three subsets: training (80%), validation, and test data (10% each). These subsets undergo various image processing techniques such as normalization, resizing, and Gaussian blur before being fed into our merged CNN with LSTM architecture. Through rigorous experimentation, we identify the optimal models—VCEPTION (VGG + Inception) and VMOBILENET (VGG + MobileNet)—for our merged CNN with LSTM framework. We introduce an X-OR gate mechanism between these models to enhance performance, ensuring consensus in disease prediction and disregarding cases where the models provide conflicting outputs. In hierarchical classification, we follow a similar procedure of dataset splitting and employ merged CNN with LSTM models. If the main class prediction indicates Lymphoma, we apply PCA followed by KNN classification. Otherwise, we proceed with the standard merged CNN with the LSTM model. This methodology, characterized by meticulous dataset handling, innovative model architectures, and strategic classification approaches, promises heightened accuracy and performance in multicancer image classification. Figure 6 illustrates the model architecture. Beginning with dataset selection, the image processing unfolds in two sections: a vertical and a horizontal side. The vertical section represents the simultaneous output model, where two CNNs process the image, merge, and then undergo LSTM processing. Subsequently, a dense layer and dropout are applied before jointly classifying the main class and subclass. Conversely, the horizontal section depicts an alternative classification approach. Here, two CNNs merge, pass through an LSTM layer, predict the main class, and, based on this main class, undergo another two merged CNNs. Another LSTM layer is then applied, enabling the model to predict specific main class subtypes.

E. APPLIED X-OR GATE AS A POST PROCESSING

Incorporating X-OR logic into a medical imaging classification system that utilizes two different models is an innovative approach aimed at enhancing diagnostic accuracy and reliability. This method addresses a critical aspect of medical diagnostics: ensuring the correct identification of diseases, as misclassification can lead to inappropriate patient management with potentially grave consequences.

The principle of the X-OR gate [30], which outputs true or high only when the inputs differ, is central to this approach. By applying X-OR logic to the predictions from two distinct

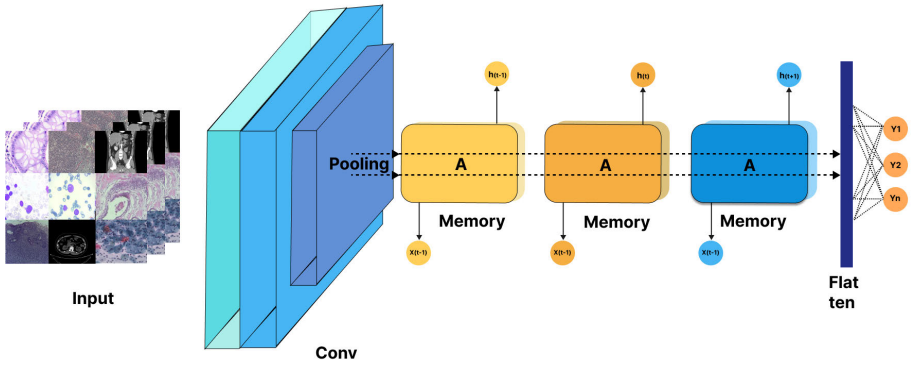

FIGURE 5. Integration of CNN with LSTM for advanced cancer detection.

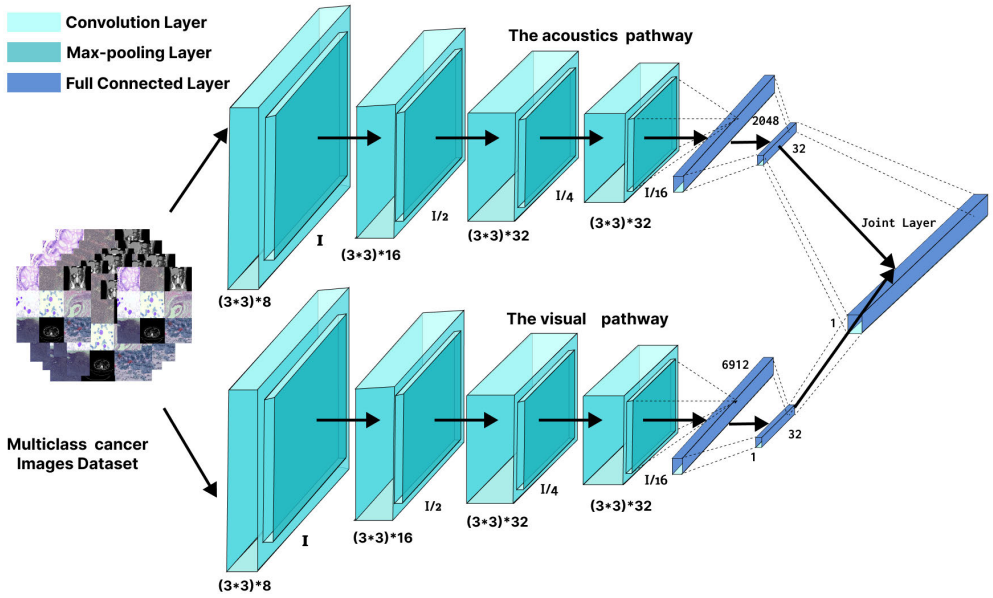

FIGURE 6. Merge CNN framework.

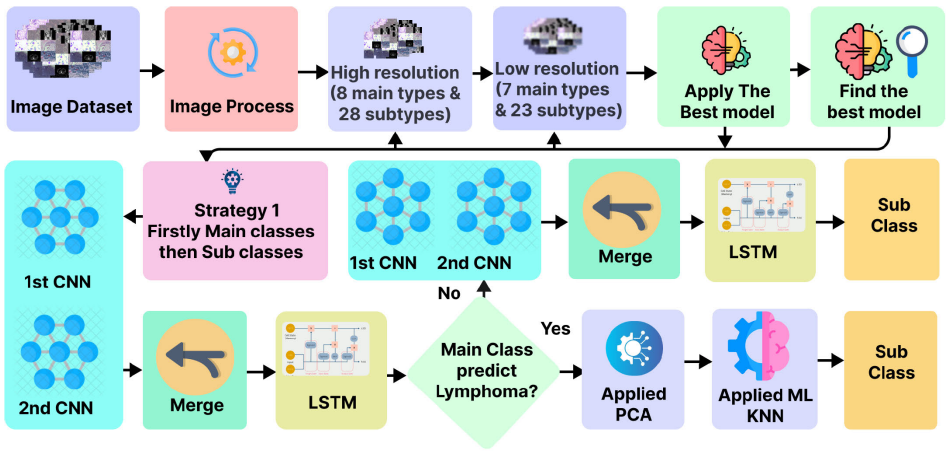

FIGURE 7. Strategy 1.

classification models for the same input image, the system can identify cases of disagreement or confusion between the models as shown in Table 4. For instance, if Model A predicts Disease 1 and Model B predicts Disease 2 for the same image, the X-OR gate would output a signal indicating a discrepancy, suggesting that the case requires further review or should

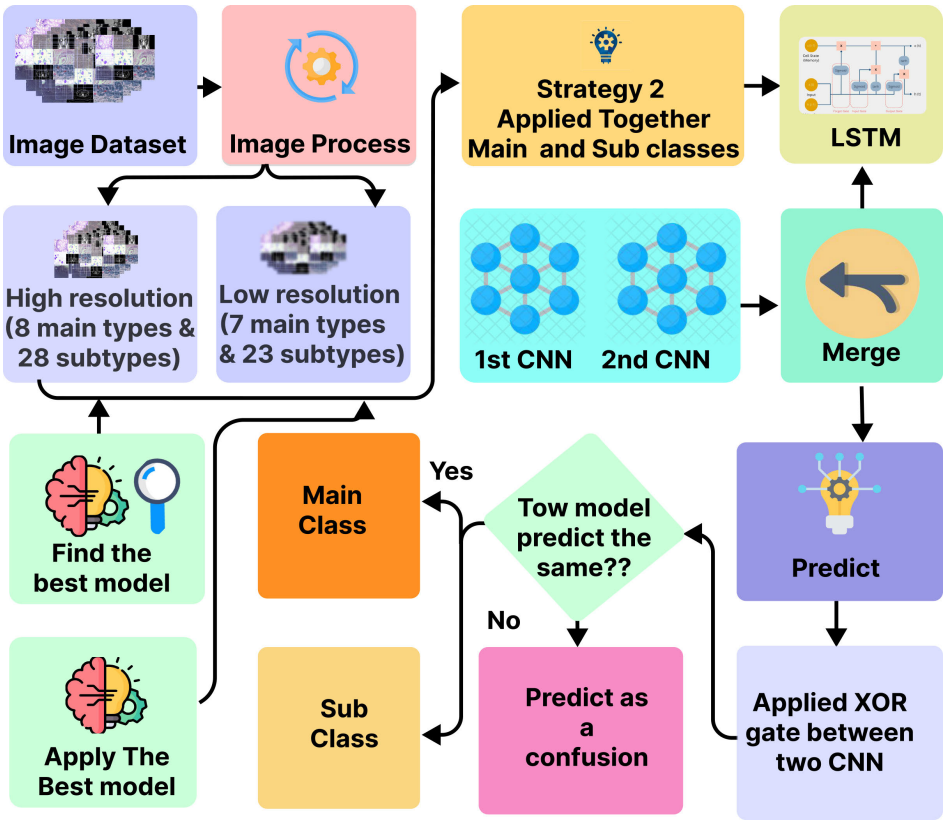

FIGURE 8. Strategy 2.

TABLE 4. X-OR output table.

Model 1	Model 2	Output
0	0	0
0	1	Confusion
1	0	Confusion
1	1	0

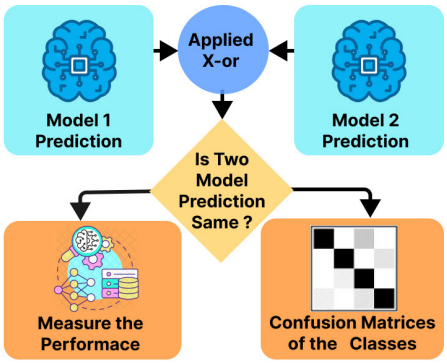

FIGURE 9. X-OR logic in medical image classification.

be classified into a confusion category. This methodology is depicted in Figure 9, which illustrates how predictions from the two models are input into an X-OR gate. The outcome of this process is either a confirmation of a consensus diagnosis (when both models agree) or a flag for further investigation

TABLE 5. Hyperparameter settings.

Method	Tuning Hyperparameters
KNN	PCA value=50, image size =(100,100,3), nearest neighbour =5
CNN	input_shape=(100,100,3), dense=(256 & 128), dropout=(0.5), optimization=(custom_adam), metrics=(accuracy, precision, recall, f1-score), loss=categorical_cross_entropy

(when the models disagree), as indicated by the X-OR gate's output. This system design significantly increases the diagnostic system's overall performance and trustworthiness by ensuring that only cases with consistent model predictions are accepted without question, thereby minimizing the risk of misdiagnosis.

F. REFINING DATA WITH DIMENSIONALITY REDUCTION VIA PCA

In dealing with high-dimensional image data, PCA serves as a critical preprocessing step, streamlining the dataset to its most informative features. This dimensionality reduction not only simplifies the computational task but also amplifies the model's focus on the most significant aspects of cancer detection. By reducing the dimensionality of the image data, PCA helps mitigate the curse of dimensionality, making the dataset more manageable for ML algorithms such as KNN, Support Vector Machine(SVM), etc.

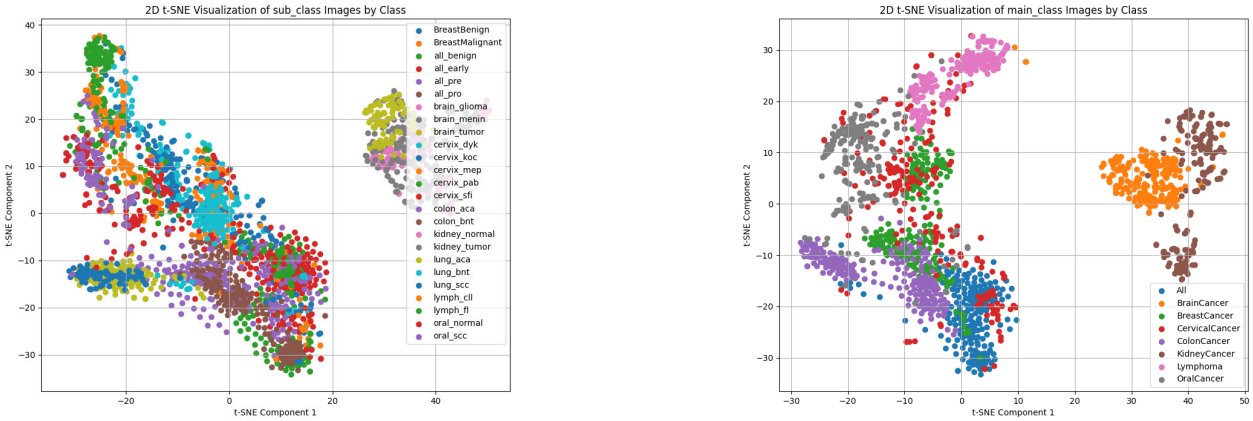

FIGURE 10. 2D t-SNE visualization main cancer and sub cancer.

TABLE 6. Model performance metrics for strategy 1.

Model Name	Main Class Acc	Sub Class Acc	Test Main Class Acc	Test Sub Class Acc
VGG16	99.504	86.078	99.813	82.539
InceptionV3	99.930	98.943	99.767	90.242
ResNet50	99.891	98.908	92.483	77.637
ResNet152	99.565	98.591	98.739	84.874
Xception	99.813	95.182	96.685	76.423
ConvNetxTiny	93.6913	62.400	89.635	52.474
ConvNetxLarge	93.578	72.134	90.756	27.731
EfficientNetB0	99.956	98.295	92.987	84.583
MobileNetV2	99.478	98.608	85.387	51.867
DenseNet201	99.860	98.552	99.346	51.867
NASNetLarge	99.478	98.713	90.021	89.246
KNN	89.07	63.42	72.69	60.14
SVM	80.04	57.01	68.56	52.45
Decision Tree	78.48	56.45	63.57	55.22

Mathematically, PCA identifies the principal components $\mathbf{v}_1, \mathbf{v}_2, \ldots, \mathbf{v}_d$, which are the eigenvectors corresponding to the largest eigenvalues of the covariance matrix Σ, capturing the maximum variance in the data. By projecting the original image data $\mathbf{X}$ onto the subspace defined by the principal components $\mathbf{V}$ using the equation

$$\mathbf{X}_{\text{PCA}} = \mathbf{X}\mathbf{V} \tag{1}$$

PCA retains the essential information while reducing the data's dimensionality, making it particularly beneficial for tasks such as skin cancer detection from dermoscopic images.

1) IMAGE IN 2D(T-SNE)

In Figure 10, we present a comprehensive visual exploration of a multicancer image dataset using t-distributed Stochastic Neighbor Embedding (t-SNE), a method renowned for its ability to effectively reduce the dimensionality of high-dimensional data for visualization. This figure artfully segregates the dataset into two distinct halves: the left side meticulously showcases the array of subclasses, while the right side brings into focus the primary cancer categories.

Figure 11 offers a closer look at eight specific cancer subtypes, including Breast Cancer, Colon Cancer, Kidney Cancer, Lymphoma, Oral Cancer, Brain Cancer, and Cervical Cancer.

G. CNN + LSTM + KNN FUSION

In our secondary classification approach, mirroring our initial methodology, we embarked on an additional investigation to delve deeper into our model's performance. We identified a discrepancy in the effectiveness of subclass classification within the Lymphoma category when employing individualized CNN analyses for each main class. To address this observation comprehensively, we extended our analysis by employing various ML models separately, including the integration of PCA. Our findings revealed that Lymphoma subclass classification exhibited superior accuracy with KNN compared to CNN-based approaches. This nuanced exploration underscores the importance of considering alternative methodologies within specific subclassifications, offering valuable insights into optimizing cancer classification strategies. In this section, we present a novel approach that combines CNN, LSTM networks, and KNN to enhance classification performance. Initial experiments involved applying distinct CNN models to each main class independently, revealing consistent success across

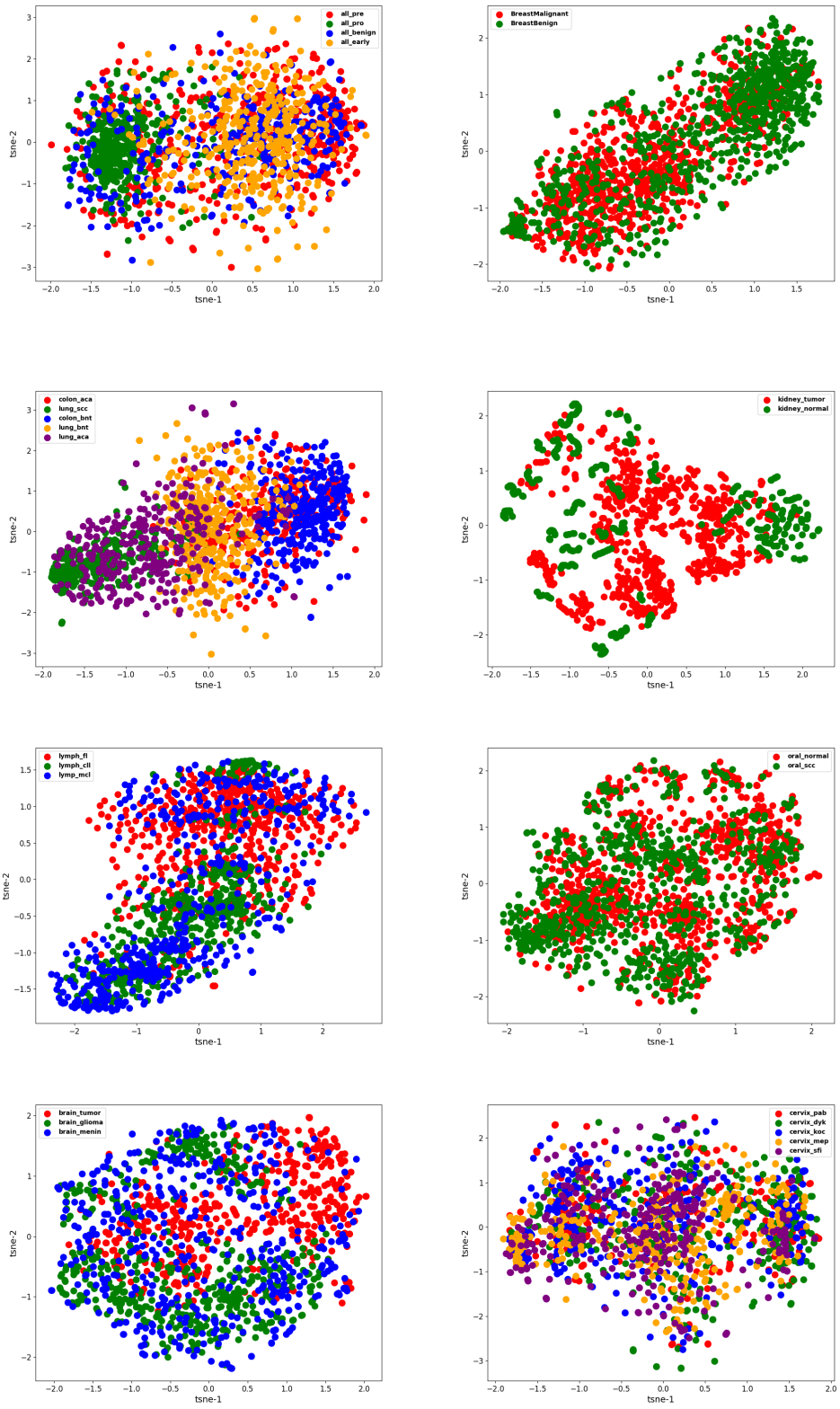

FIGURE 11. t-SNE visualization of multicancer image data.

most classes, except for Lymphoma, where CNN exhibited suboptimal accuracy. To address this challenge, we propose a multi-stage approach. We first merge the CNN with LSTM for the initial prediction of the main class. If Lymphoma is identified as the primary prediction, we further refine the classification using PCA combined with KNN. Conversely,

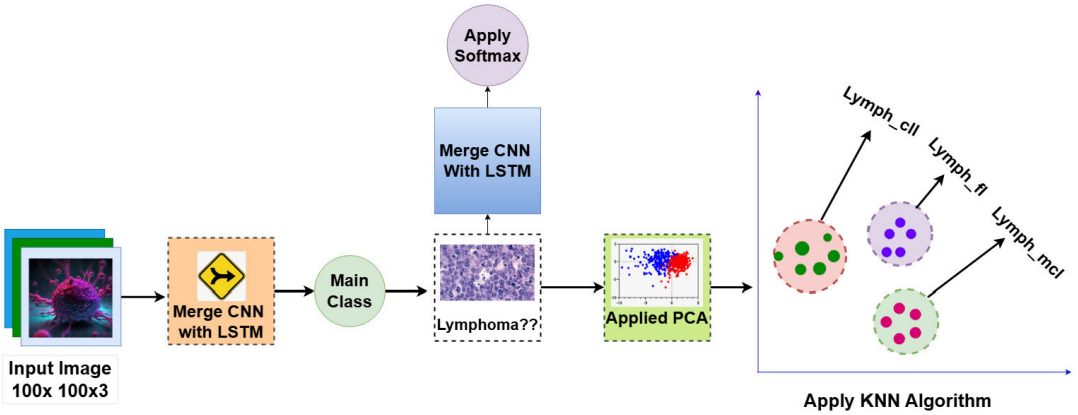

FIGURE 12. Illustration of the integrated CNN-LSTM-KNN architecture.

TABLE 7. Model performance metrics with KNN for strategy 1.

Model Name	Main Class Acc	Sub CLass Acc	Test Main Class Acc	Test Sub Class Acc
VGG + KNN	87.46	81.31	85.51	78.87
Inception + KNN	90.38	85.22	85.76	80.41
ResNet + KNN	88.67	81.26	82.81	80.44
Xception + KNN	89.33	80.24	84.41	75.39
MobileNet + KNN	89.82	84.36	85.74	80.50

TABLE 8. Model performance metrics - combined CNNs for strategy 2.

Model	Main Class Acc	Sub Class Acc	Test Main Class Acc	Test Sub Class Acc
VGG + ResNet	99.36	97.31	98.06	97.21
Inception + ResNet	99.10	96.67	98.31	95.50
VGG + Xception	99.42	85.40	94.83	84.44
Inception + Xception	99.17	92.23	97.86	90.38
VGG + inception	99.73	97.29	98.82	96.43

TABLE 9. Model performance metrics - combined models for strategy 2.

Model	Main Class Acc	Sub CLass Acc	Test Main Class Acc	Test Sub Class Acc
VGG + ResNet+LSTM	99.21	95.67	97.36	94.56
VGG + Inception +LSTM	**99.83**	**97.41**	**99.13**	**97.80**
VGG + Xception+LSTM	99.63	97.63	99.13	97.40
VGG + MobileNet+LSTM	**99.81**	**97.78**	**99.25**	**97.66**
MobileNet + Inception +LSTM	99.75	07.29	98.82	96.77

for classes other than Lymphoma, the input is directed through an alternative CNN with LSTM. In addition to the CNN-LSTM-KNN architecture, we explore the integration of PCA with various traditional ML models, including DT, SVM, and KNN. Interestingly, the PCA-KNN combination exhibits superior performance specifically for Lymphoma compared to other pre-trained CNN models. To visually represent our proposed architecture, refer to Figure 12. This Figure illustrates the sequential flow of information through the integrated CNN, LSTM, and KNN model, showcasing decision points where Lymphoma triggers the secondary PCA-KNN pathway, while other classes proceed through an alternative CNN-LSTM route. The mathematical representation [31] of KNN shows:

$$\hat{y}_q = \text{argmax}_y \sum_{\mathbf{x}_i \in \mathcal{N}_q} \mathbb{I}(y_i = y) \tag{2}$$

where,
- $\hat{y}_q$: Predicted class label for data point $\mathbf{x}_q$.
- $\mathcal{N}_q$: Set of k nearest neighbors of $\mathbf{x}_q$.
- y_i: Class label of data point $\mathbf{x}_i$ in the training dataset $\mathcal{D}$.
- $\mathbb{I}(\cdot)$: Indicator function that returns 1 if the condition is true and 0 otherwise.

H. HYPERPARAMETER SETTING

The custom Adam optimizer extends the standard Adam algorithm to accommodate specific optimization requirements [32]. One potential modification involves introducing an additional regularization term into the parameter update rule to mitigate overfitting [33]. The custom Adam update rule with regularization is given by:

$$m_t = \beta_1 m_{t-1} + (1 - \beta_1) g_t,$$
$$v_t = \beta_2 v_{t-1} + (1 - \beta_2) g_t^2,$$

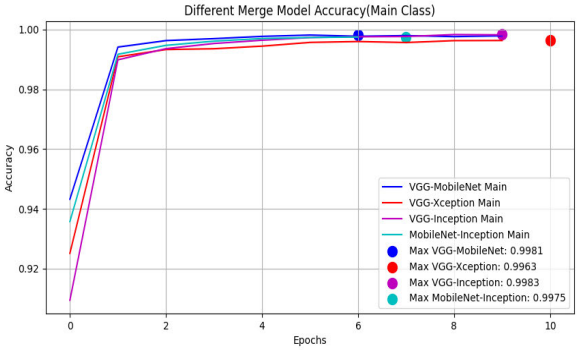

(a) Different merge model accuracy (main class)

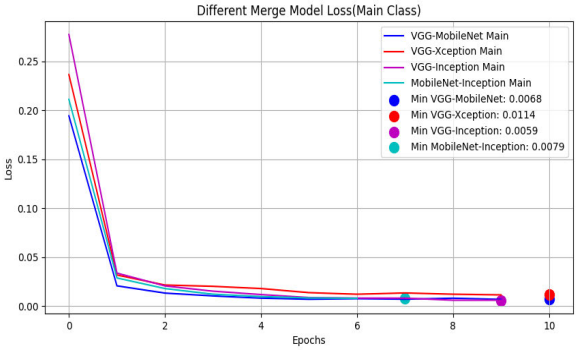

(c) Different merge model loss (main class)

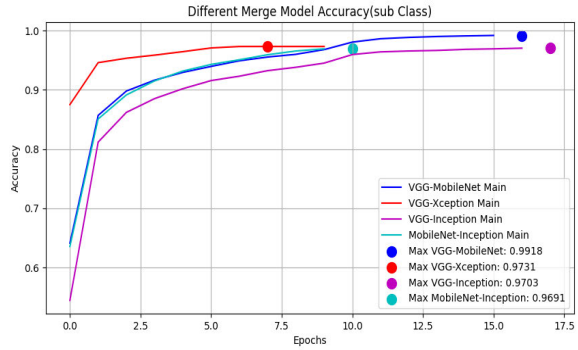

(b) Different merge model accuracy (subclass)

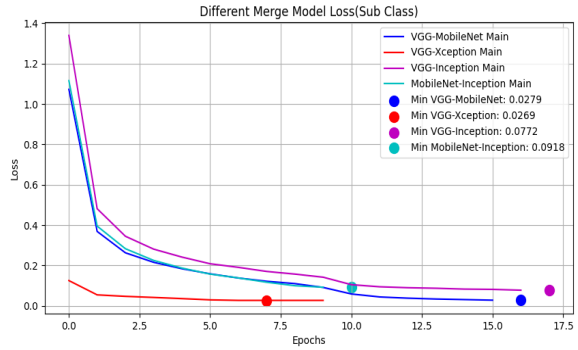

(d) Different merge model loss (subclass)

FIGURE 13. Different merge model accuracy and loss for main and sub class.

TABLE 10. Lymphoma and subclass accuracy using various models with PCA.

Model	Lymphoma	lymp_mcl	lymph_cll	lymp_fl
CNN	95.21%	97.31	96.06	93.21
CNN with LSTM	95.85%	97.07	94.31	95.50
SVM	88.21%	84.13	88.16	90.44
KNN	**97.14%**	**98.17**	**97.86**	**96.38**
Decision Tree	91.73%	92.29	90.82	92.43

TABLE 11. Classification report for main class by Vmobilenet.

Class	Precision	Recall	F1-Score	Support
BrainCancer	1.00	1.00	1.00	2047
OralCancer	1.00	1.00	1.00	1549
CervicalCancer	0.99	0.98	0.99	981
ALL	1.00	1.00	1.00	2401
Lymphoma	1.00	1.00	1.00	1020
KidneyCancer	1.00	1.00	1.00	2517
ColonCancer	1.00	1.00	1.00	1003
BreastCancer	0.97	1.00	0.99	483
Accuracy			1.00 (12001)	
Macro Avg			1.00	
Weighted Avg			1.00	

$$\hat{m}_t = \frac{m_t}{1-\beta_1^t},$$
$$\hat{v}_t = \frac{v_t}{1-\beta_2^t},$$
$$\theta_t = \theta_{t-1} - \alpha\left(\frac{\hat{m}_t}{\sqrt{\hat{v}_t}+\epsilon} + \lambda R(\theta_{t-1})\right). \quad (3)$$

where α is the learning rate, β_1 and β_2 are exponential decay rates for moment estimates, g_t is the gradient of the loss function, ϵ is a small constant for numerical stability, λ is the regularization parameter, and $R(\theta_{t-1})$ is a regularization function applied to the model parameters θ.

Table 5 provides a comprehensive overview of the hyperparameter settings utilized in the experimental configuration for the KNN and CNN classification methods. For KNN, parameters such as PCA value, image size, and the number of nearest neighbors are specified, while for CNN, details encompass input shape, dense layer configurations, dropout rate, optimization strategy, and evaluation metrics. These hyperparameter choices are pivotal in fine-tuning the models for optimal performance, particularly in medical image analysis tasks like skin cancer detection, where accuracy and reliability are paramount.

IV. RESULT AND DISCUSSION

Table 6 shows how different ML models perform in image classification tasks, giving a clear picture of their strengths and weaknesses. DL models such as InceptionV3 and EfficientNetB0 exhibit superior performance, particularly in

TABLE 12. Classification report for main class by Vception.

Class	Precision	Recall	F1-Score	Support
BrainCancer	1.00	1.00	1.00	2047
OralCancer	1.00	1.00	1.00	1549
CervicalCancer	0.98	0.95	0.97	981
ALL	1.00	1.00	1.00	2401
Lymphoma	1.00	1.00	1.00	1020
KidneyCancer	0.99	0.99	0.99	2517
ColonCancer	0.99	1.00	0.99	1003
BreastCancer	0.96	1.00	0.98	483
Accuracy		0.99 (12001)		
Macro Avg		0.99		
Weighted Avg		0.99		

TABLE 13. Classification report for main class after applying X-OR gate in two models.

Class	Precision	Recall	F1-Score	Support
All	1.00	1.00	1.00	2394
BrainCancer	1.00	1.00	1.00	2044
BreastCancer	1.00	1.00	1.00	480
CervicalCancer	1.00	1.00	1.00	919
ColonCancer	1.00	1.00	1.00	998
KidneyCancer	1.00	1.00	1.00	2497
Lymphoma	1.00	1.00	1.00	1020
OralCancer	1.00	1.00	1.00	1549
Accuracy		1.00		11901
Macro Avg	1.00	1.00	1.00	11901
Weighted Avg	1.00	1.00	1.00	11901

handling sub-class accuracy, which is a testament to their robust feature extraction and generalization capabilities. The Table also highlights the challenges faced by custom convolutional networks, such as ConvNetxTiny and ConvNetxLarge, which lag behind the more sophisticated pre-trained models in both main and sub-class accuracy metrics. Furthermore, traditional ML models like KNN, SVM, and DT show significantly lower performance, underscoring the advantage of DL models in complex visual recognition tasks. This comparative analysis emphasizes the importance of model selection based on the specific requirements of the classification task and the nature of the dataset, highlighting the need for further research into optimization strategies to enhance model performance and generalizability across diverse tasks.

Table 7 investigates the efficacy of combining KNN with various CNN models for multicancer classification. The study introduces hybrid models, notably **Inception + KNN** and **MobileNet + KNN**, to utilize the DL capabilities of CNNs alongside the simplicity and interpretability of KNN.

Table 8 showcases the performance metrics of various combined CNN models for an unspecified classification task. The combinations include **VGG + ResNet**, **Inception + ResNet**, **VGG + Xception**, **Inception + Xception**, and **ResNet + Xception**. These models are evaluated based on four key metrics: Main Class Accuracy, Sub Class Accuracy, Test Main Class Accuracy, and Test Sub Class Accuracy. The table reveals a general trend where combining different CNN architectures results in varied performance outcomes,

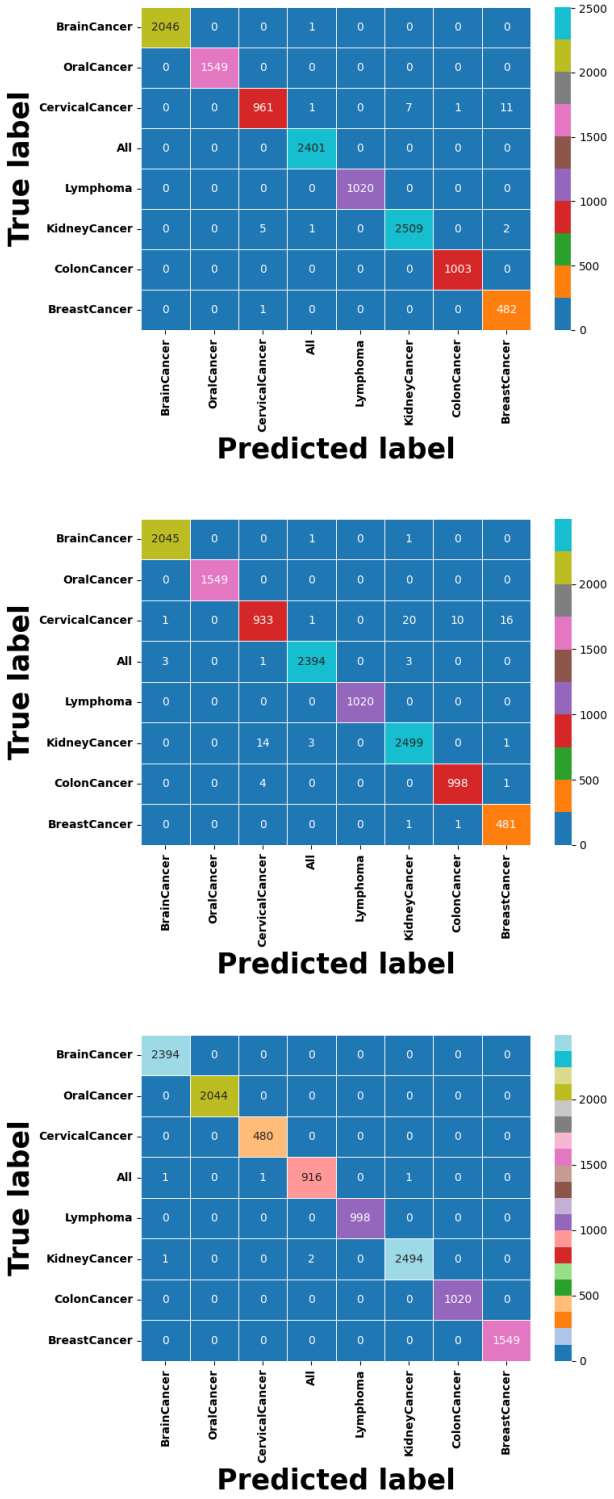

FIGURE 14. Confusion matrices (a)Vmobilenet main class (b)Vception main class (c)After applying X-OR gate for the main class before and after applying the X-OR gate.

with **Inception + ResNet** showing the highest Main Class Accuracy on both training and test data. However, the Sub Class Accuracies are notably lower across all combinations,

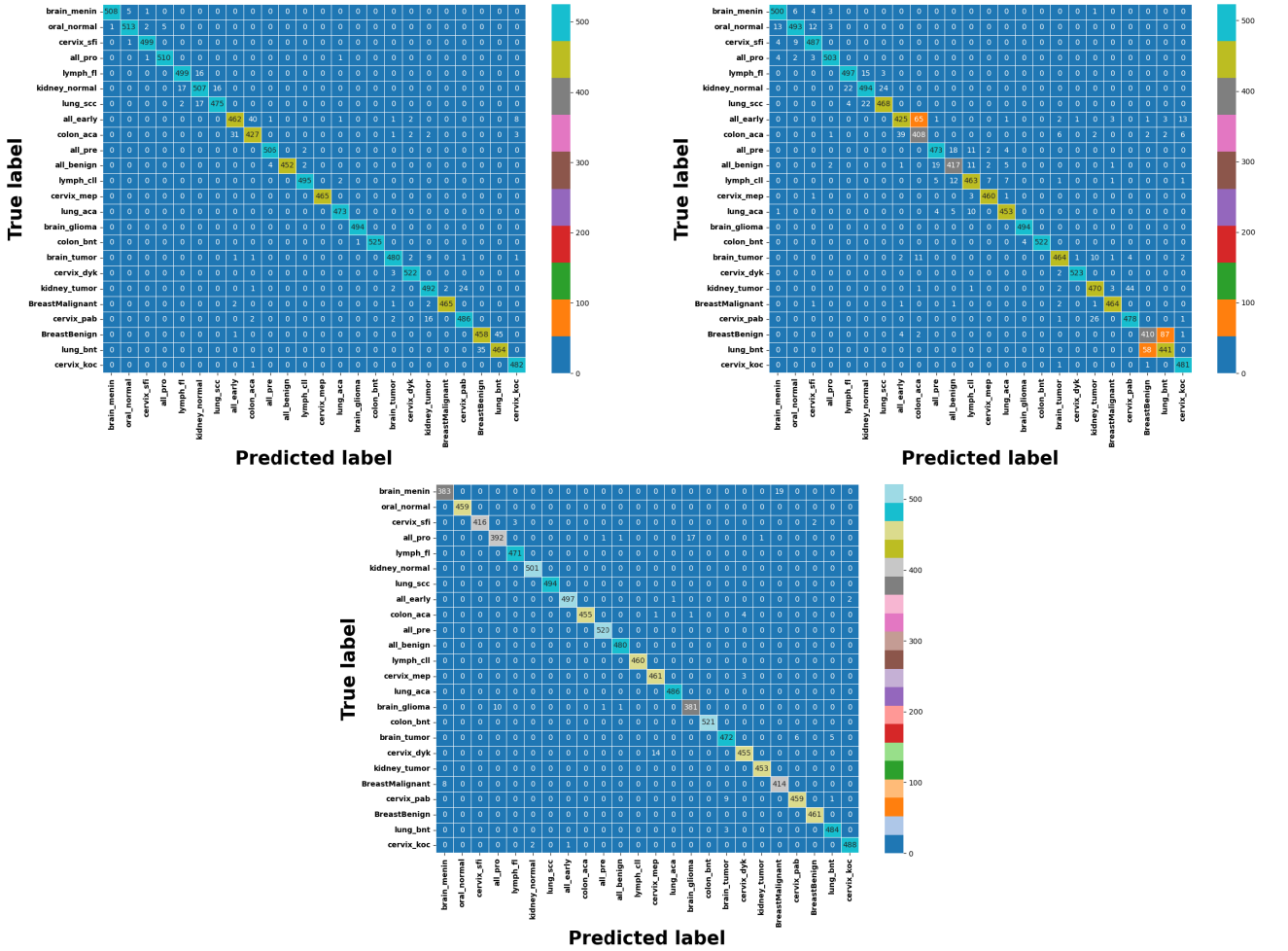

FIGURE 15. Confusion matrices (a)Vmobilenet subclass (b)Vception subclass (c)After applying X-OR gate for the subclass before and after applying the X-OR gate.

suggesting challenges in capturing the finer distinctions within classes. This analysis highlights the potential and limitations of architecturally diverse CNN combinations in enhancing model performance for complex classification tasks.

Table 9 summarizes the performance of various combinations of DL models, which merge LSTM networks with popular CNN architectures such as VGG, ResNet, Inception, Xception, and MobileNet. The combination of VGG + Inception + LSTM, in particular, distinguishes itself by securing the highest accuracies in test scenarios for both category levels, achieving 99.13% and 97.80%, respectively. This indicates that merging LSTM with CNN models successfully harnesses spatial and sequential data attributes, thereby bolstering the models' predictive performance on new data.

Figure 13 illustrates the variations in merge model accuracy and loss graphs for both the main class and subclass. Additionally, it showcases the maximum accuracy gain and minimum loss values achieved by each merge model within 20 epochs. Notably, the merge models "VGG-Inception" and "VGG-MobileNet" exhibit particularly impressive accuracy results. Specifically, for the main class classification, "VGG-Inception" achieves an outstanding accuracy of 99.83% and 99.81% with corresponding loss values of 0.0059 and 0.0068, respectively. These values underscore the exceptional performance of "VGG-Inception" in accurately classifying main class labels.

A. ACCURACY OF LYMPHOMA

As CNN exhibits lower accuracy in the classification of Lymphoma for strategy 1 in Figure7, our study delves into the classification accuracies of various ML models applied to both Lymphoma and its subclasses. Emphasizing the role of PCA, we investigate its impact on model performance using the top 50 pixels extracted from medical images. The results presented in Table 10 highlight the robustness and effectiveness of the KNN model, achieving an impressive accuracy of 97.14% for Lymphoma classification.

TABLE 14. Classification report for subclass by Vmobilenet.

Class	Precision	Recall	F1-Score	Support
brain_menin	1.00	0.99	0.99	514
oral_normal	0.99	0.98	0.99	521
cervix_sfi	0.99	1.00	1.00	500
all_pro	0.99	1.00	0.99	512
lymph_fl	0.96	0.97	0.97	515
kidney_normal	0.94	0.94	0.94	540
lung_scc	0.97	0.96	0.96	494
all_early	0.93	0.90	0.91	515
colon_aca	0.90	0.92	0.91	466
all_pre	0.99	1.00	0.99	508
all_benign	1.00	0.99	0.99	458
lymph_cll	0.99	1.00	0.99	497
cervix_mep	1.00	1.00	1.00	465
lung_aca	0.99	1.00	1.00	473
brain_glioma	1.00	1.00	1.00	494
colon_bnt	1.00	1.00	1.00	526
brain_tumor	0.98	0.97	0.97	495
cervix_dyk	0.99	0.99	0.99	525
kidney_tumor	0.94	0.94	0.94	521
BreastMalignant	1.00	0.99	0.99	470
cervix_pab	0.95	0.96	0.96	506
BreastBenign	0.93	0.91	0.92	504
lung_bnt	0.91	0.93	0.92	499
cervix_koc	0.98	1.00	0.99	483
Accuracy		0.976 (12001)		

TABLE 15. Classification report for subclass by Vception.

Class	Precision	Recall	F1-Score	Support
brain_menin	0.96	0.97	0.97	514
oral_normal	0.97	0.95	0.96	521
cervix_sfi	0.96	0.97	0.97	500
all_pro	0.98	0.98	0.98	512
lymph_fl	0.95	0.97	0.96	515
kidney_normal	0.93	0.91	0.92	540
lung_scc	0.95	0.95	0.95	494
all_early	0.90	0.83	0.86	515
colon_aca	0.84	0.88	0.86	466
all_pre	0.94	0.93	0.94	508
all_benign	0.92	0.91	0.92	458
lymph_cll	0.93	0.93	0.93	497
cervix_mep	0.98	0.99	0.98	465
lung_aca	0.96	0.96	0.96	473
brain_glioma	0.99	1.00	1.00	494
colon_bnt	1.00	0.99	1.00	526
brain_tumor	0.96	0.94	0.95	495
cervix_dyk	1.00	1.00	1.00	525
kidney_tumor	0.92	0.90	0.91	521
BreastMalignant	0.98	0.99	0.98	470
cervix_pab	0.91	0.94	0.93	506
BreastBenign	0.97	0.94	0.84	504
lung_bnt	0.97	0.96	0.95	499
cervix_koc	0.95	1.00	0.97	483
Accuracy		0.978 (12001)		

TABLE 16. Classification report for subclass after applying X-OR gate in two models.

Class	Precision	Recall	F1-Score	Support
BreastBenign	0.98	0.95	0.97	402
BreastMalignant	1.00	1.00	1.00	459
all benign	1.00	0.99	0.99	421
all early	0.98	0.95	0.96	412
all pre	0.99	1.00	1.00	471
all pro	1.00	1.00	1.00	501
brain glioma	1.00	1.00	1.00	494
brain menin	1.00	0.99	1.00	500
brain tumor	1.00	0.99	0.99	461
cervix dyk	1.00	1.00	1.00	520
cervix koc	1.00	1.00	1.00	480
cervix mep	1.00	1.00	1.00	460
cervix pab	0.97	0.99	0.98	464
cervix sfi	1.00	1.00	1.00	486
colon aca	0.95	0.97	0.96	393
colon bnt	1.00	1.00	1.00	521
kidney normal	0.98	0.98	0.98	483
kidney tumor	0.98	0.97	0.98	469
lung aca	1.00	1.00	1.00	453
lung bnt	0.96	0.98	0.97	422
lung scc	0.99	0.98	0.98	469
lymph cll	1.00	1.00	1.00	461
lymph fl	0.99	0.99	0.99	487
oral normal	1.00	0.99	0.99	491
Accuracy		0.9918 (11180)		

This improvement is particularly striking in the KNN model, surpassing other models across all subclasses. This underscores the KNN model's potential for accurate and reliable Lymphoma classification.

B. EFFECT OF X-OR GATE AT STRATEGY 2

Our research meticulously evaluated the two best CNN models, Vmobilenet and Vception, for cancer classification. At first, the two models did not reach the highest accuracy. But after adding an X-OR gate later, their accuracy and precision greatly improved. This strategy resulted in notable enhancements in both main and subclass classifications, as evidenced by the confusion matrices. The X-OR gate's implementation refined accuracy by leveraging the combined strengths of the individual models. This led to a decrease in misclassifications and improved clarity in class differentiation. Notably, the X-OR gate had a substantial impact on precision, recall, and F1 scores, highlighting the advantage of merging models to address the complexities of cancer detection tasks. Our study conclusively shows that integrating an X-OR gate between two CNN models not only addresses individual model limitations but also outperforms our proposed model in accuracy. This underscores the effectiveness of our approach in enhancing the reliability and precision of medical diagnostics, specifically in cancer classification.

Figures 14 and 15 illustrate the confusion matrices for both the main and subclass classifications before and after the application of the X-OR gate. The implementation of the X-OR gate led to a main class accuracy nearing 99.95%, a substantial improvement over the initial accuracies of 99.25% for Vmobilenet and 99.83% for Vception. Similarly, for the subclass, accuracies of 97.66% and 97.80% were observed for Vmobilenet and Vception, respectively, which, after applying the X-OR gate, increased to 99.13%. These results underscore the efficacy of combining models through X-OR logic in enhancing the precision of medical image classification.

Following this, The Tables accompanying this study provide a comprehensive insight into the classification performance of the Vmobilenet and Vception models, both individually and after integrating an X-OR gate. Table 11 and Table 14 detail the classification reports for the main and

TABLE 17. State of the art on cancer diagnosis.

Ref	Model Used	Learning Type	Cancer Types	Accuracy
[16]	CNN	DL	ALL	95.54%
[17]	Residual Networks	DL	Brain cancer	99%
[18]	CNN with LSTM	DL	Breast cancer	97.2%
[19]	Neural Network	DL	Cervical cancer	95.1%
[20]	CNN	DL	Kidney cancer	99.92%
[21]	CNN (ResNet, UNet, SegNet)	Transfer Learning	Lung and Colon Cancer	96.98%
[22]	Multiple CNNs	DL	Lymphoma	100%
[23]	EfficientNet-B0	Transfer Learning	Oral Cancer	85.0%
Our proposed model	**VCEPTION and VMOBILENET**	**DL**	**All types of cancer**	**99.25%,97.80%**

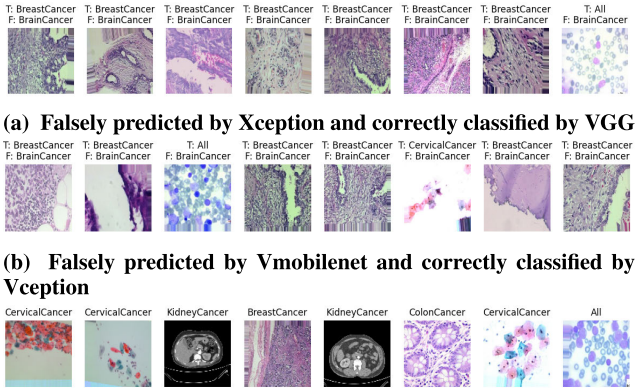

(a) Falsely predicted by Xception and correctly classified by VGG

(b) Falsely predicted by Vmobilenet and correctly classified by Vception

(c) Misclassified cases: false predictions by both models

FIGURE 16. False images before applying X-OR gate.

sub-classes using the Vmobilenet model, respectively. Similarly, Table 12 and Table 15 present the performance metrics for the Vception model. Notably, the strategic application of an X-OR gate to combine the outputs of these models resulted in marked improvements, as highlighted in Table 13 and 16. These Tables showcase enhanced accuracy, precision, recall, and F1 scores, further substantiating the efficacy of model ensembling techniques in complex classification tasks.

In Figure 16, three subfigures illustrate the comparative performance of the Vmobilenet and Vception models in image classification tasks. Subfigure 16a shows images that were misclassified by Vception but correctly identified by Vmobilenet, highlighting the instances where Vmobilenet outperforms Vception. Conversely, Subfigure 16b includes images accurately classified by Vmobilenet but not by Vception, indicating similar discriminative capabilities between the models. Lastly, Subfigure 16c depicts images that both models failed to classify correctly, underscoring the challenges or limitations faced by each model in certain scenarios. This arrangement effectively demonstrates the strengths and weaknesses of each model in processing and recognizing various image types.

C. COMPARISON WITH STATE-OF-THE-ART STUDIES FOR STRATEGY 2

For a fair comparison, we evaluated the performance scores of our novel proposal against state-of-the-art methods. This review encompassed a broad spectrum of cutting-edge methods developed in the past year. As shown in Table 17, other models primarily focus on a single class of cancer, whereas our model targets eight different types of cancer and their subtypes. The accuracy of our proposed model is 99.25% for main classes and 97.80% for sub-classes.

V. CONCLUSION AND FUTURE WORK

In this study, we developed a novel approach for enhancing the accuracy and reliability of multiple cancer detection using images. We combined CNN models with LSTM networks and applied PCA and KNN, finding PCA and KNN together sometimes outperformed CNNs. The rigorous evaluation showed our methodology improved accuracy, precision, recall, and F1-scores for cancer classifications. Post-processing with an X-OR gate between models also enhanced performance, even when individual model accuracy was not high. Our findings highlight the potential of ensemble learning and logical operations in complex classification tasks. However, challenges remain, such as accurately classifying main and subclass cancer types together due to independent nodes, which may lead to contradictory classifications. Additionally, using an X-OR gate introduces a "confusion section" for difficult-to-classify images, and the hierarchical classification process can mislead subclass predictions if the main class is incorrectly predicted.

In our study, we applied two different approaches to cancer classification, revealing significant shortcomings. For instance, the model might predict a main class and a subclass that are inherently contradictory due to their independent classification nodes—such as identifying the main class as brain cancer but the subclass as belonging to cervical cancer. In our study, we found a challenging part when working with an X-OR gate that made it hard to deal with some images. Out of the 12,001 images we tested, we couldn't easily classify 100 main categories and 821 subcategories because they were unclear. This brings up the issue of how to handle these uncertain cases. Also, our method first tries to figure out the main category of an image before identifying the more specific subcategory related to that main category. This approach can lead to incorrect subclass predictions if the main class is wrongly identified, given the subclass's dependence on the main class accuracy. In future work, we aim to address these limitations to enhance the reliability and coherence of our cancer classification model.

ACKNOWLEDGMENT

The authors would like to acknowledge Princess Nourah bint Abdulrahman University Researchers Supporting Project number (PNURSP2024R197), Princess Nourah bint Abdulrahman University, Riyadh, Saudi Arabia. The authors would like to thank Prince Sultan University for their support.

REFERENCES

[1] M. Nahiduzzaman, L. F. Abdulrazak, M. A. Ayari, A. Khandakar, and S. M. R. Islam, "A novel framework for lung cancer classification using lightweight convolutional neural networks and ridge extreme learning machine model with Shapley additive explanations (SHAP)," *Expert Syst. Appl.*, vol. 248, Aug. 2024, Art. no. 123392.

[2] I. Houda, C. Dickhoff, C. A. Uyl-de Groot, R. A. M. Damhuis, N. Reguart, M. Provencio, A. Levy, R. Dziadziuszko, C. Pompili, M. D. Maio, M. Thomas, A. Brunelli, S. Popat, S. Senan, and I. Bahce, "Challenges and controversies in resectable non-small cell lung cancer: A clinician's perspective," *Lancet Regional Health—Eur.*, 2024.

[3] S. Saeedi, S. Rezayi, H. Keshavarz, and S. R. Niakan Kalhori, "MRI-based brain tumor detection using convolutional deep learning methods and chosen machine learning techniques," *BMC Med. Informat. Decis. Making*, vol. 23, no. 1, p. 16, Jan. 2023.

[4] K. K. Anilkumar, V. J. Manoj, and T. M. Sagi, "A review on computer aided detection and classification of leukemia," *Multimedia Tools Appl.*, vol. 83, no. 6, pp. 17961–17981, Jul. 2023.

[5] P. K. Das, D. V. A. S. Meher, R. Panda, and A. Abraham, "A systematic review on recent advancements in deep and machine learning based detection and classification of acute lymphoblastic leukemia," *IEEE Access*, vol. 10, pp. 81741–81763, 2022.

[6] H. Abolhassani, A. Eskandari, A. Saremi Poor, A. Zarrabi, B. Khodadadi, S. Karimifard, H. Sahrayi, M. Bourbour, and M. Tavakkoli Yaraki, "Nanobiotechnological approaches for breast cancer management: Drug delivery systems and 3D in-vitro models," *Coordination Chem. Rev.*, vol. 508, Jun. 2024, Art. no. 215754.

[7] M. F. Ak, "A comparative analysis of breast cancer detection and diagnosis using data visualization and machine learning applications," *Healthcare*, vol. 8, no. 2, p. 111, Apr. 2020.

[8] F. R. Burdier, D.-E.-N. Waheed, B. Nedjai, R. D. M. Steenbergen, M. Poljak, M. Baay, A. Vorsters, and S. Van Keer, "DNA methylation as a triage tool for cervical cancer screening—A meeting report," *Preventive Med. Rep.*, vol. 41, May 2024, Art. no. 102678.

[9] M. M. Kalbhor and S. V. Shinde, "Cervical cancer diagnosis using convolution neural network: Feature learning and transfer learning approaches," *Soft Comput.*, Jul. 2023, doi: 10.1007/s00500-023-08969-1.

[10] K. Rajkumar, R. T. Sri Ramoju, T. Balelly, S. Ashadapu, C. R. Prasad, and Y. Srikanth, "Kidney cancer detection using deep learning models," in *Proc. 7th Int. Conf. Trends Electron. Informat. (ICOEI)*, Apr. 2023, pp. 1197–1203.

[11] H. A. Mengash, M. Alamgeer, M. Maashi, M. Othman, M. A. Hamza, S. S. Ibrahim, A. S. Zamani, and I. Yaseen, "Leveraging marine predators algorithm with deep learning for lung and colon cancer diagnosis," *Cancers*, vol. 15, no. 5, p. 1591, 2023.

[12] E. A. M. Zijtregtop, L. A. Winterswijk, T. P. A. Beishuizen, C. M. Zwaan, R. A. J. Nievelstein, F. A. G. Meyer-Wentrup, and A. Beishuizen, "Machine learning logistic regression model for early decision making in referral of children with cervical lymphadenopathy suspected of lymphoma," *Cancers*, vol. 15, no. 4, p. 1178, Feb. 2023.

[13] H. Myriam, A. A. Abdelhamid, E. M. El-Kenawy, A. Ibrahim, M. M. Eid, M. M. Jamjoom, and D. S. Khafaga, "Advanced meta-heuristic algorithm based on particle swarm and al-biruni Earth radius optimization methods for oral cancer detection," *IEEE Access*, vol. 11, pp. 23681–23700, 2023.

[14] J. Dubroff, D. Johnson, and H. Botha, "State of art of molecular imaging in the diagnosis and treatment of dementia," *Amer. J. Geriatric Psychiatry*, vol. 32, no. 4, p. 31, Apr. 2024.

[15] Y. Xue, S. Chen, J. Qin, Y. Liu, B. Huang, and H. Chen, "Application of deep learning in automated analysis of molecular images in cancer: A survey," *Contrast Media Mol. Imag.*, vol. 2017, pp. 1–10, Jun. 2017.

[16] N. Sampathila, K. Chadaga, N. Goswami, R. P. Chadaga, M. Pandya, S. Prabhu, M. G. Bairy, S. S. Katta, D. Bhat, and S. P. Upadya, "Customized deep learning classifier for detection of acute lymphoblastic leukemia using blood smear images," *Healthcare*, vol. 10, no. 10, p. 1812, Sep. 2022.

[17] S. A. Abdelaziz Ismael, A. Mohammed, and H. Hefny, "An enhanced deep learning approach for brain cancer MRI images classification using residual networks," *Artif. Intell. Med.*, vol. 102, Jan. 2020, Art. no. 101779.

[18] J. Zheng, D. Lin, Z. Gao, S. Wang, M. He, and J. Fan, "Deep learning assisted efficient AdaBoost algorithm for breast cancer detection and early diagnosis," *IEEE Access*, vol. 8, pp. 96946–96954, 2020.

[19] S. Cheng et al., "Robust whole slide image analysis for cervical cancer screening using deep learning," *Nature Commun.*, vol. 12, no. 1, p. 5639, Sep. 2021.

[20] L. B. da Cruz, J. D. L. Araujo, J. L. Ferreira, J. O. B. Diniz, A. C. Silva, J. D. S. de Almeida, A. C. de Paiva, and M. Gattass, "Kidney segmentation from computed tomography images using deep neural network," *Comput. Biol. Med.*, vol. 123, Aug. 2020, Art. no. 103906.

[21] A. Ben Hamida, M. Devanne, J. Weber, C. Truntzer, V. Derangère, F. Ghiringhelli, G. Forestier, and C. Wemmert, "Deep learning for colon cancer histopathological images analysis," *Comput. Biol. Med.*, vol. 136, Sep. 2021, Art. no. 104730.

[22] D. Li, J. R. Bledsoe, Y. Zeng, W. Liu, Y. Hu, K. Bi, A. Liang, and S. Li, "A deep learning diagnostic platform for diffuse large B-cell lymphoma with high accuracy across multiple hospitals," *Nature Commun.*, vol. 11, no. 1, p. 6004, Nov. 2020.

[23] F. Jubair, O. Al-karadsheh, D. Malamos, S. A. Mahdi, Y. Saad, and Y. Hassona, "A novel lightweight deep convolutional neural network for early detection of oral cancer," *Oral Diseases*, vol. 28, no. 4, pp. 1123–1130, May 2022.

[24] O. S. Naren. (2022). *Multi Cancer Dataset: 8 Types of Cancer Images*. [Online]. Available: https://www.kaggle.com/datasets/obulisainaren/multi-cancer

[25] L. Fu, J. Zhu, W. Li, Q. Zhu, B. Xu, Y. Xie, Y. Zhang, Y. Hu, J. Lu, P. Dang, and J. You, "Tunnel vision optimization method for VR flood scenes based on Gaussian blur," *Int. J. Digit. Earth*, vol. 14, no. 7, pp. 821–835, Jul. 2021.

[26] R. Valand, S. Tanna, G. Lawson, and L. Bengtström, "A review of Fourier transform infrared (FTIR) spectroscopy used in food adulteration and authenticity investigations," *Food Addit Contaminants, Part A*, vol. 37, no. 1, pp. 19–38, Jan. 2020.

[27] M. S. Islam, M. A. T. Rony, and T. Sultan, "GastroVRG: Enhancing early screening in gastrointestinal health via advanced transfer features," *Intell. Syst. Appl.*, vol. 23, Sep. 2024, Art. no. 200399.

[28] J. O. Bappi, M. A. T. Rony, and M. S. Islam, "BNVGLENET: Hypercomplex Bangla handwriting character recognition with hierarchical class expansion using convolutional neural networks," *Natural Lang. Process. J.*, vol. 7, Jun. 2024, Art. no. 100068.

[29] M. S. Islam and M. A. T. Rony, "CDK: A novel high-performance transfer feature technique for early detection of osteoarthritis," *J. Pathol. Informat.*, vol. 15, Dec. 2024, Art. no. 100382.

[30] R. Sardar, A. Nandi, A. Bhowmik, B. Dutta, and S. Ghosh, "Design of EX-OR gate with ANN using sigmoid and ReLu functions for artificial intelligence applications in Python," in *Proc. Int. Conf. Data Anal. Insights*, 2023, pp. 779–789.

[31] S. Zhang, "Challenges in KNN classification," *IEEE Trans. Knowl. Data Eng.*, vol. 34, no. 10, pp. 4663–4675, Oct. 2022.

[32] R. B. Sarooraj and S. Prayla Shyry, "Analysis of traffic flow prediction from spatial–temporal data using hybrid GSA-adam optimizer based LSTM network for intelligent transport system," *Multimedia Tools Appl.*, vol. 83, no. 6, pp. 16735–16761, Jul. 2023.

[33] A. D. Viniski, J. P. Barddal, A. de Souza Britto, and H. V. A. de Campos, "Incremental specialized and specialized-generalized matrix factorization models based on adaptive learning rate optimizers," *Neurocomputing*, vol. 552, Oct. 2023, Art. no. 126515.

JABED OMAR BAPPI received the B.Sc. degree in electrical and electronics engineering from the Department of Electrical and Electronic Engineering (EEE), Port City International University, Chittagong, Bangladesh, in 2022. His current research interests include data science, artificial intelligence, data mining, natural language processing, ML, DL, and image processing.

MOHAMMAD ABU TAREQ RONY received the B.Sc. degree in statistics from Noakhali Science and Technology University, Noakhali, Bangladesh. In addition, he possesses expertise in devising advanced analytics strategies using data. His diverse professional experience includes four years of research in areas, such as artificial intelligence. He is currently a Research Data Scientist at aiQuest Intelligence, Dhaka, Bangladesh. Moreover, he actively engages in partnerships with international researchers, recognizing that research plays an indispensable role in fostering innovation. Overall, he is hardworking and has taught himself various skills, such as NLP, LLM, and Deep Learning. He has published articles in refereed journals and conference proceedings, such as IEEE Access, Elsevier, Springer, MDPI, and International Conferences.

MOHAMMAD SHARIFUL ISLAM received the B.Sc. degree in computer science and telecommunication engineering from Noakhali Science and Technology University, Bangladesh, in 2023, with a focus on a deep passion for cutting-edge technologies to the research community. His academic journey, rooted in the confluence of computer science and telecommunications, has evolved into a fervent pursuit of specialized areas, including data science, machine learning, natural language processing, and image processing. His work in these fields is driven by a quest to uncover hidden insights within data, develop intelligent learning algorithms, bridge the communication gap between humans and machines, and artistically enhance digital imagery. As a researcher, his approach is characterized by a blend of technical proficiency and creative problem-solving, aiming to contribute significantly to the frontiers of technology and its application in understanding and improving their digital world.

SAMAH ALSHATHRI received the bachelor's degree in computer science and the master's degree in computer engineering from King Saud University, Riyadh, Saudi Arabia, and the Ph.D. degree from the Department of Computer and Mathematics, Plymouth University, Plymouth, U.K. She is currently an Assistant Professor with the Department of Information Technology, College of Computer and Information Sciences, Princess Nourah Bint Abdulrahman University (PNU), Riyadh. Her research interests include wireless networks, cloud computing, fog computing, the IoT, data mining, machine learning, text analytics, image classification, and deep learning. She was the Chair of the Network and Communication Department and participated in organizing many international conferences. She has authored or coauthored many articles published in well-known journals in the research field.

WALID EL-SHAFAI (Senior Member, IEEE) was born in Alexandria, Egypt. He received the B.Sc. degree (Hons.) in electronics and electrical communication engineering from the Faculty of Electronic Engineering (FEE), Menoufia University, Menouf, Egypt, in 2008, the M.Sc. degree from Egypt–Japan University of Science and Technology (E-JUST), in 2012, and the Ph.D. degree from FEE, Menoufia University, in 2019. Since January 2021, he has been a Postdoctoral Research Fellow with the Security Engineering Laboratory (SEL), Prince Sultan University (PSU), Riyadh, Saudi Arabia. He is currently a Senior Cybersecurity Researcher with SEL and an Assistant Professor with the College of Computer Science and Information Systems. He is also an Associate Professor with the Department of Electronics and Communication Engineering (ECE), Faculty of Electronic Engineering, Menoufia University. His research interests include wireless mobile and multimedia communications systems, image and video signal processing, efficient 2D video/3D multi-view video coding, multi-view video plus depth coding, 3D multi-view video coding and transmission, quality of service and experience, digital communication techniques, cognitive radio networks, adaptive filters design, 3D video watermarking, steganography, encryption, error resilience and concealment algorithms for H.264/AVC, H.264/MVC, and H.265/HEVC video codecs standards, cognitive cryptography, medical image processing, speech processing, security algorithms, software-defined networks, the Internet of Things, medical diagnoses applications, FPGA implementations for signal processing algorithms and communication systems, cancellable biometrics and pattern recognition, image and video magnification, artificial intelligence for signal processing algorithms and communication systems, modulation identification and classification, image and video super-resolution and denoising, cybersecurity applications, malware and ransomware detection and analysis, deep learning in signal processing, and communication systems applications. He also serves as a reviewer for several international journals.